Electronic Supplementary Material (ESI) for Journal of Materials Chemistry A.
This journal is © The Royal Society of Chemistry 2023

Electronic Supplementary Information (ESI)

For

Thermochromic smart windows with broad-range customizable responsive temperature via the Hofmeister effect

Hongchao Peng[1], Xuekun Yang[1], Yingchun Gu[1], Qin Yang[1], Tu Lan[2,*], Sheng Chen[1,*], Bin Yan[1,*]

[1] National Engineering Laboratory for Clean Technology of Leather Manufacture, College of Biomass Science and Engineering, Sichuan University, Chengdu, 610065, China

[2] Key Laboratory of Radiation Physics and Technology of the Ministry of Education, Institute of Nuclear Science and Technology, Sichuan University, Chengdu, 610065, China

[*] Corresponding authors: tlan720@scu.edu.cn (T. L.), chensheng@scu.edu.cn (S. C.), yanbinscu@126.com (B. Y.)

Table of Contents

Figure S1. 4

Figure S2. 4

Figure S3. 5

Figure S4. 5

Figure S5. 6

Figure S6. 6

Figure S7. 7

Figure S8. 7

Figure S9. 8

Figure S10. 8

Figure S11. 9

Figure S12. 9

Figure S13. 10

Figure S14. 10

Figure S15. 11

Figure S16. 11

Figure S17. 12

Figure S18. 12

Figure S19. 13

Figure S20. 13

Figure S21. 14

Figure S22. 14

Figure S23. 15

Figure S24. 15

Figure S25. 16

Figure S26. 16

Figure S27. 17

Table S1. 18

Table S2. 19

Table S3. 20

Supplementary Figures

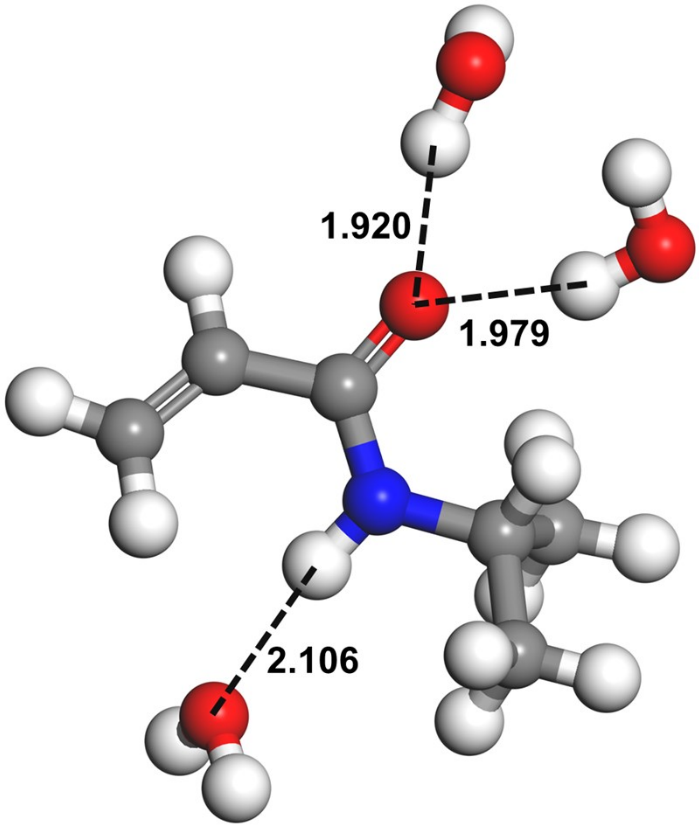

Figure S1. H-bonds formed between the NIPAM monomer and H_2O and their corresponding length.

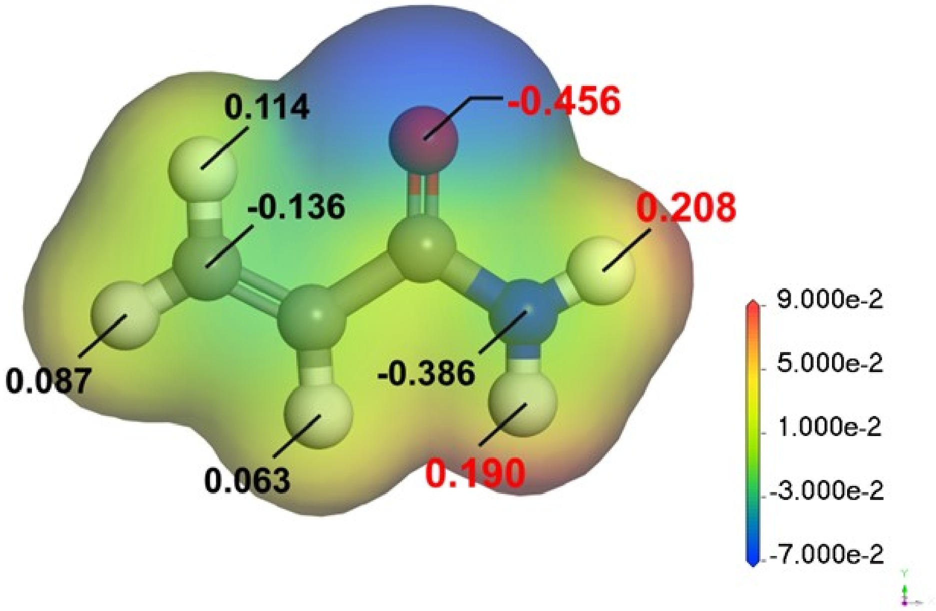

Figure S2. Electrostatic potential distribution of AM monomer.

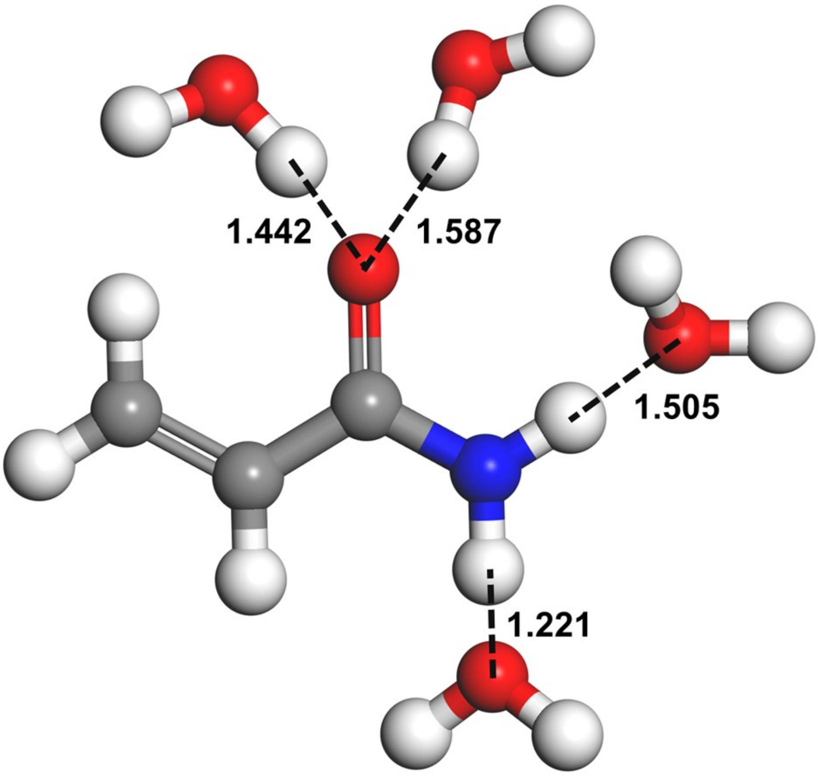

Figure S3. H-bonds formed between the AM monomer and H_2O and their corresponding length.

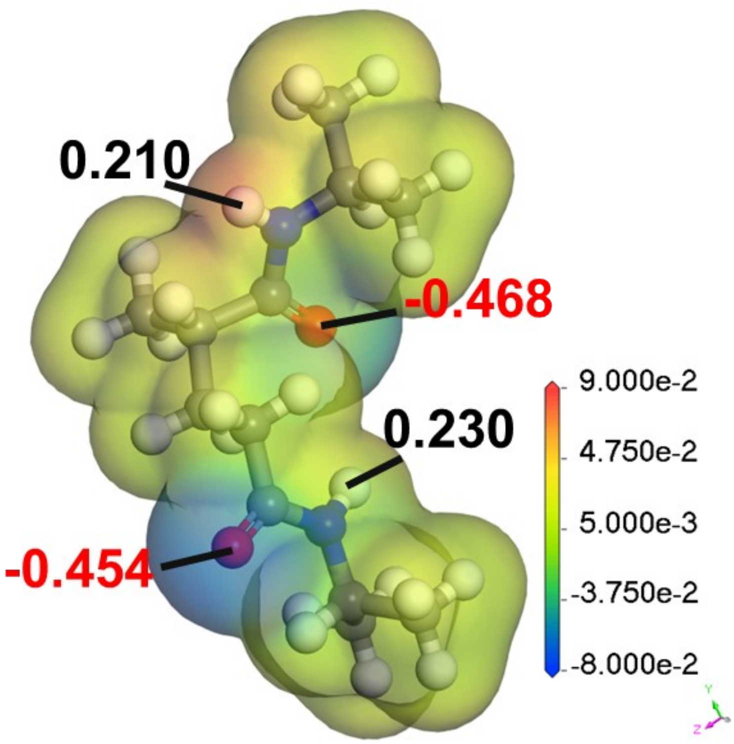

Figure S4. Electrostatic potential distribution diagram of $PNIPAM_2$.

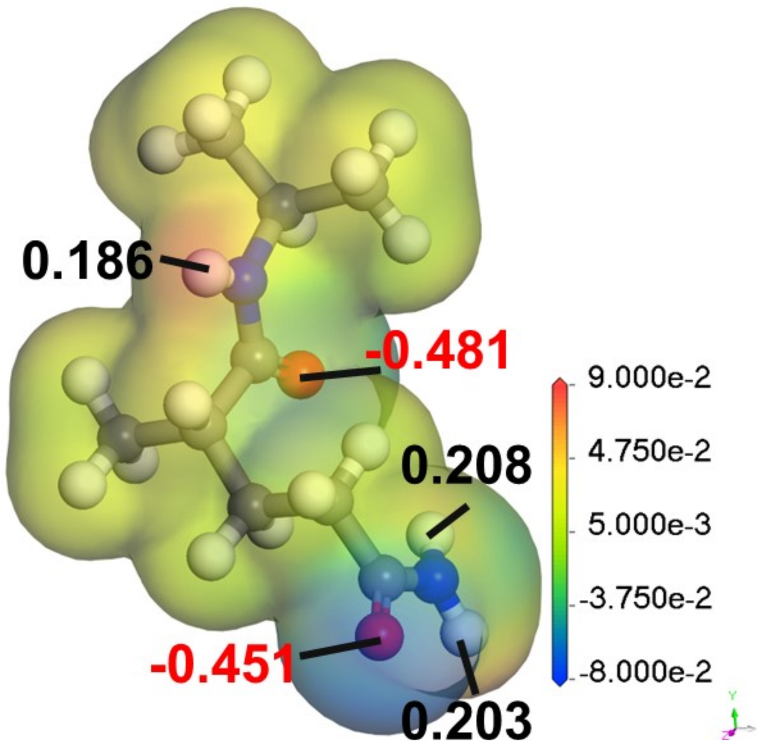

Figure S5. Electrostatic potential distribution diagram of P(NIPAM-AM)$_2$.

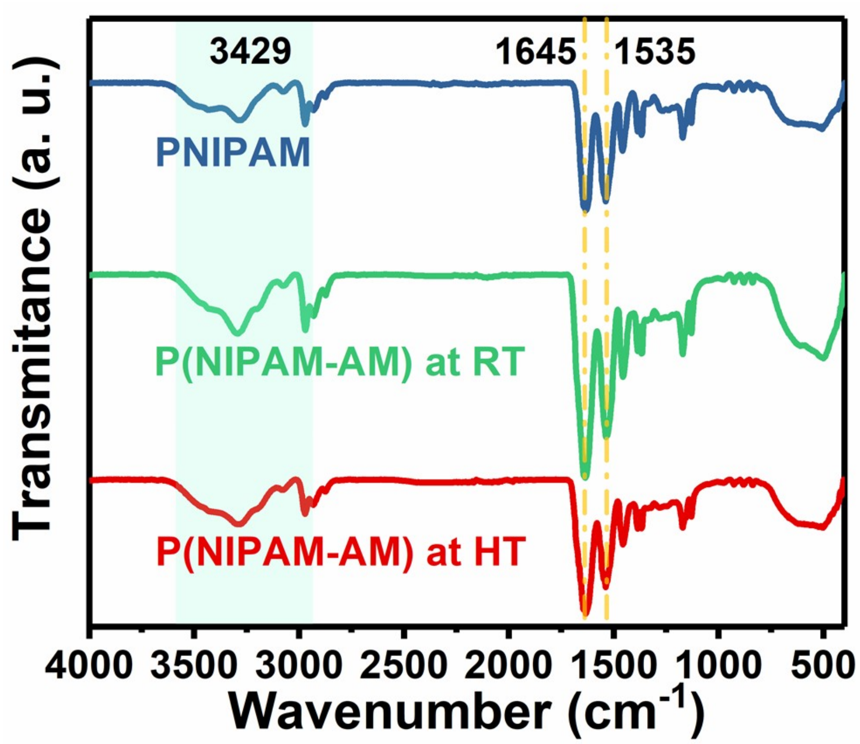

Figure S6. FTIR spectra of PNIPAM and P(NIPAM-AM) copolymer.

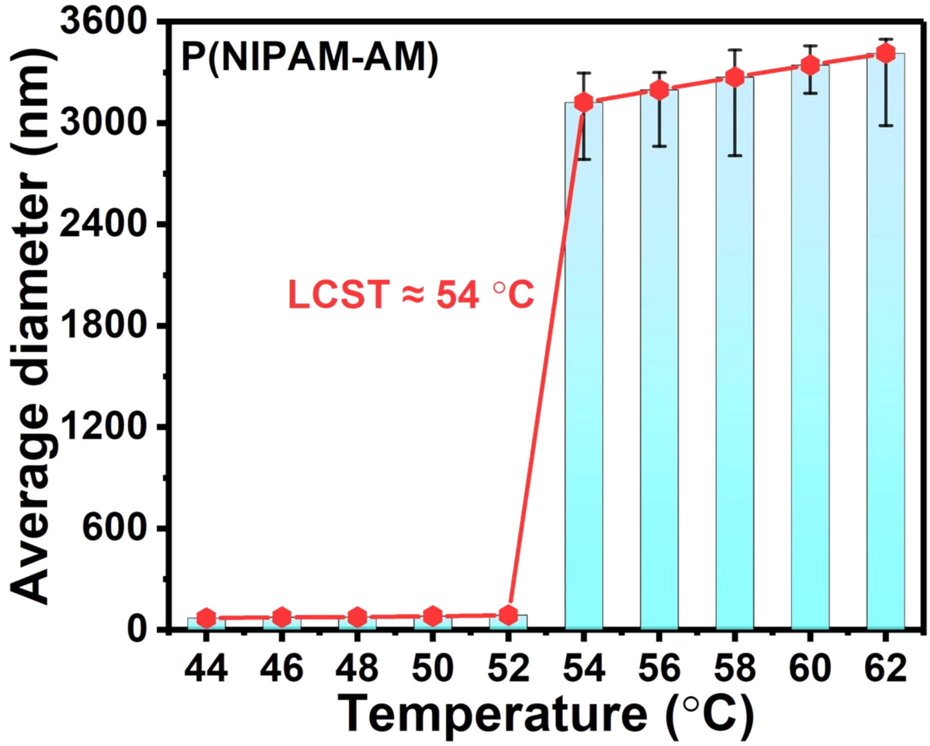

Figure S7. Dynamic light scattering tests of P(NIPAM-AM) at different temperatures.

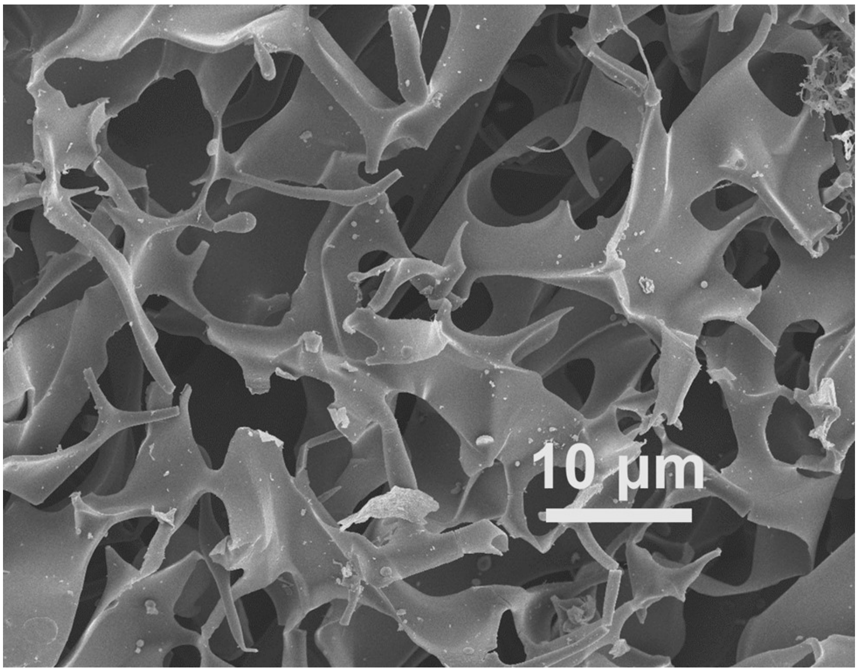

Figure S8. SEM image of PNIPAM at RT.

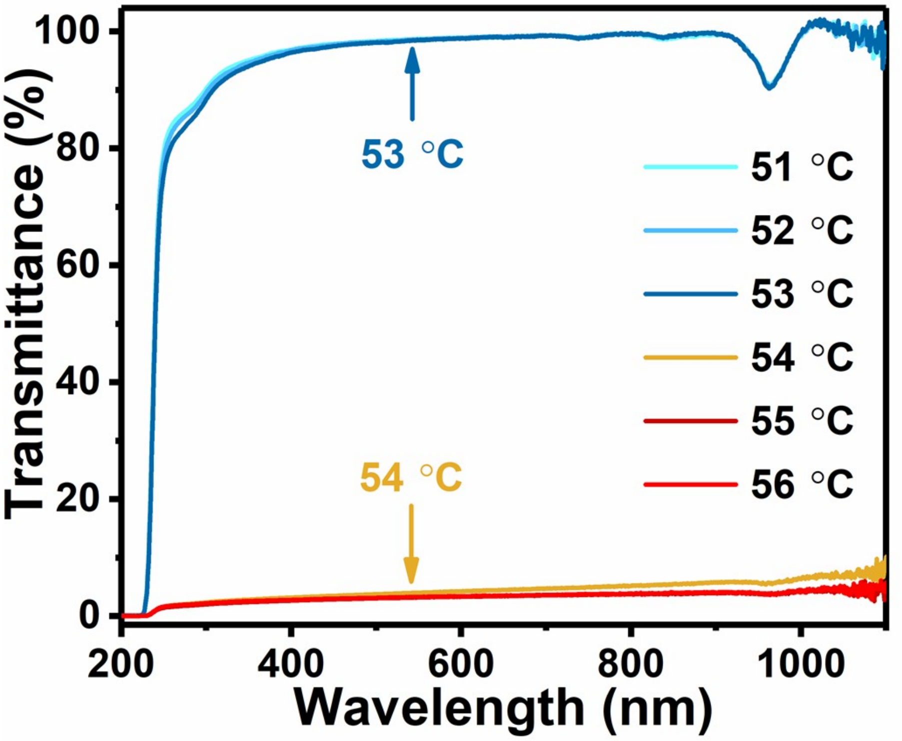

Figure S9. Transmittance spectra of PNASW at different temperatures.

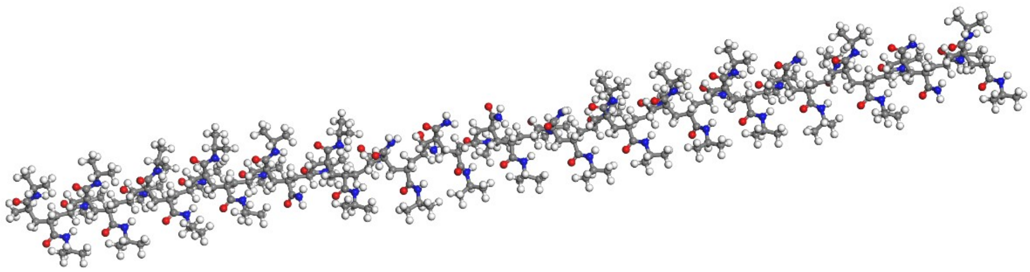

Figure S10. Geometrically optimized P(NIPAM-AM) chain.

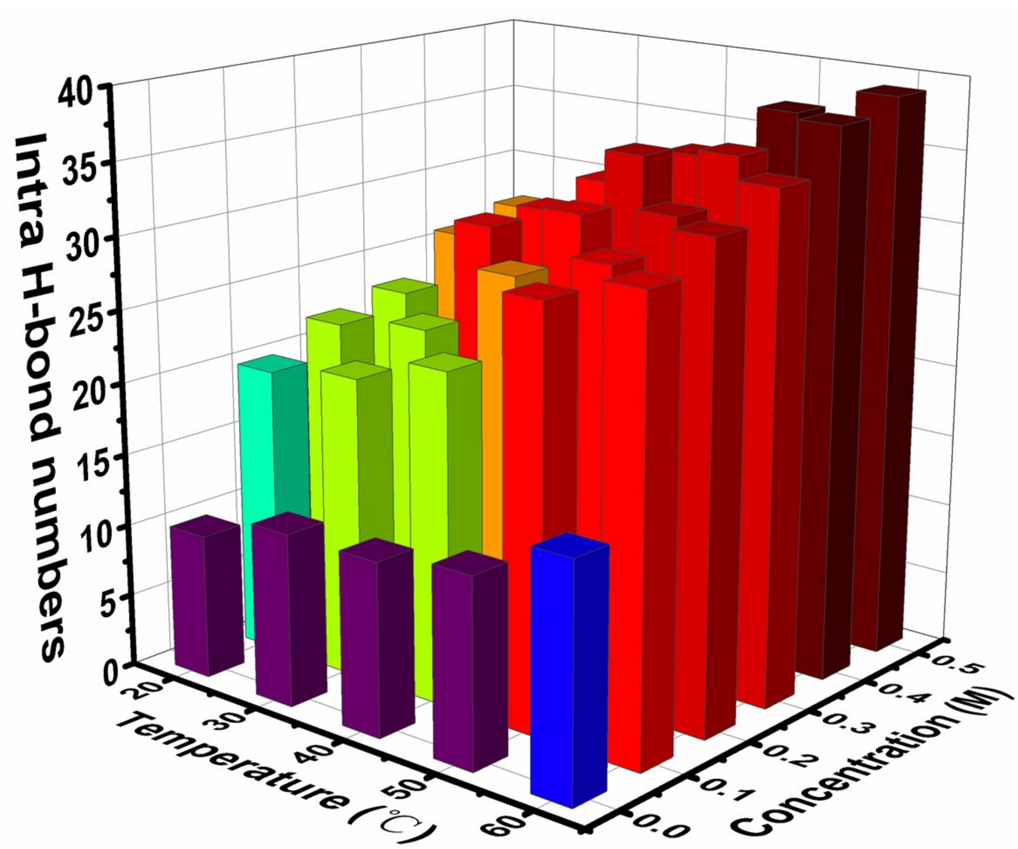

Figure S11. The number of intramolecular H-bonds varies with the temperature and concentration of Na_2SO_4.

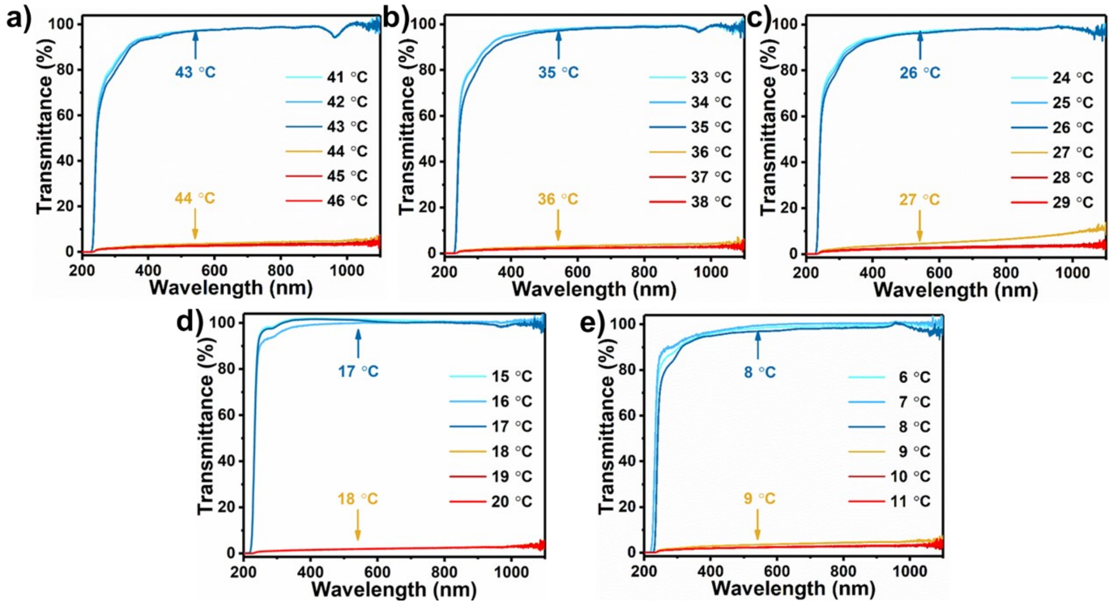

Figure S12. Transmittance-temperature spectra of PNASW with a concentration of Na_2SO_4 of a) 0.1 M, b) 0.2 M, c) 0.3 M, d) 0.4 M, and e) 0.5 M, respectively.

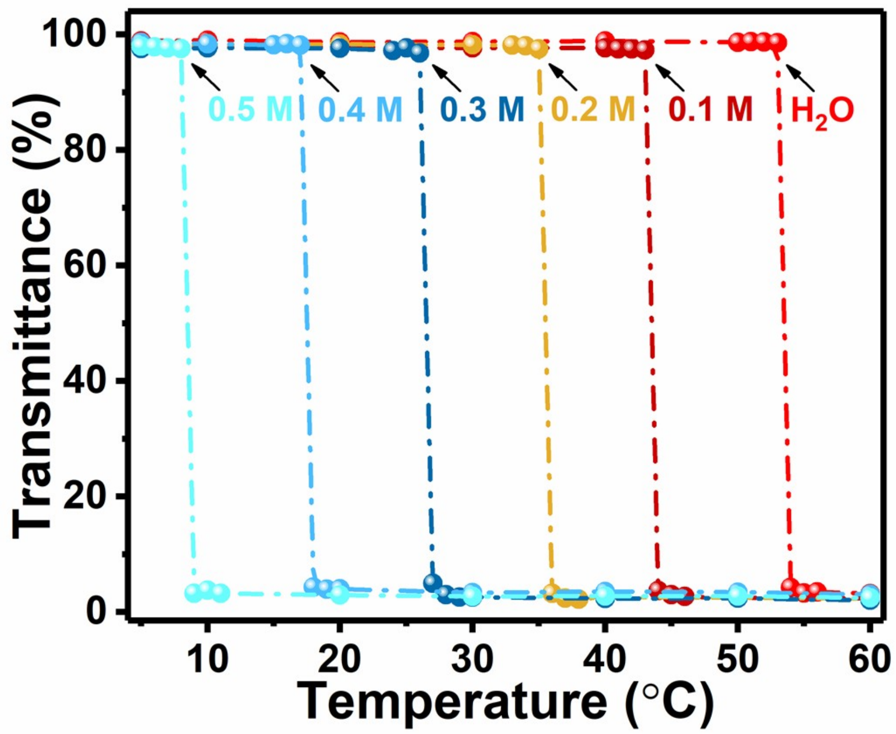

Figure S13. Transmittance-temperature responsive curves of PNASW with different concentrations of Na_2SO_4 at the wavelength of 660 nm.

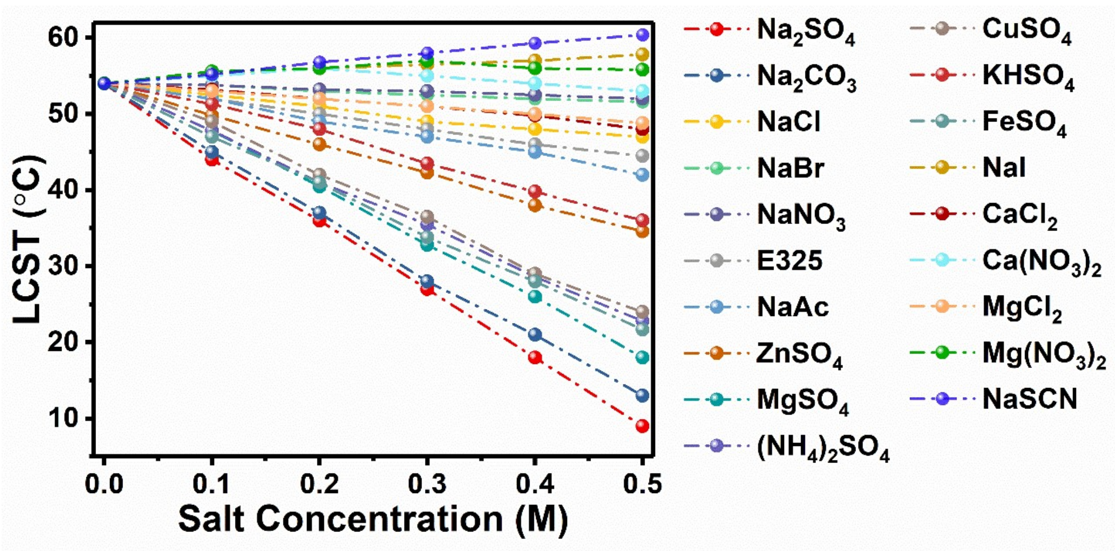

Figure S14. LCST values of P(NIPAM-AM) measured for different salts at concentrations from 0 to 0.5 M.

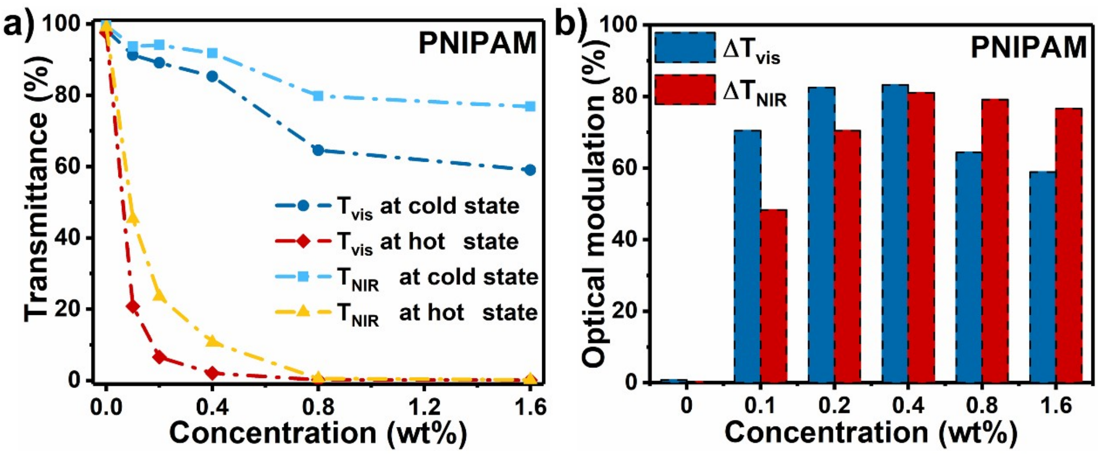

Figure S15. a) Transmittance spectra of visible and near-infrared light of PNIPAM-based smart window; b) Optical modulation of visible and near-infrared light for PNIPAM-based smart window.

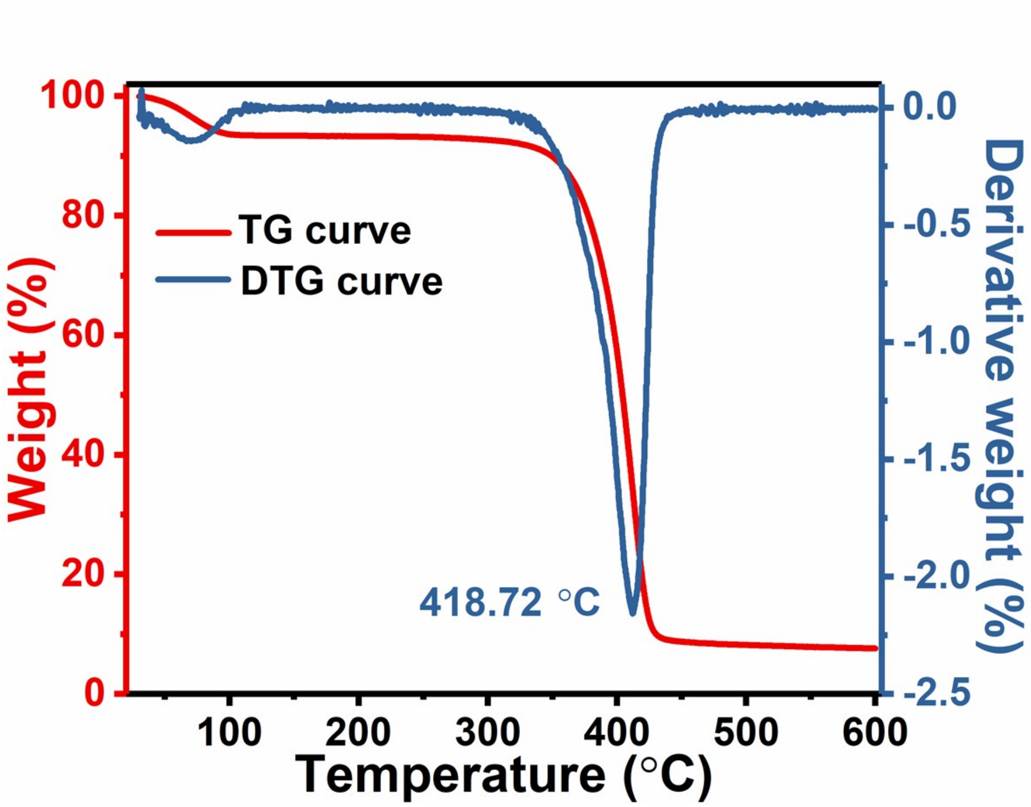

Figure S16. TG and DTG curves of P(NIPAM-AM).

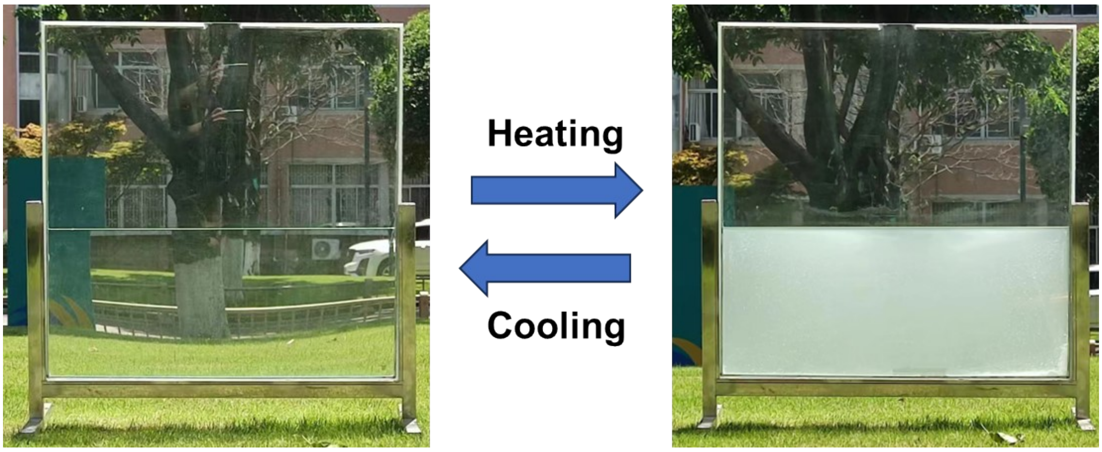

Figure S17. Optical photos of the PNASW after the durability testing of 10 months

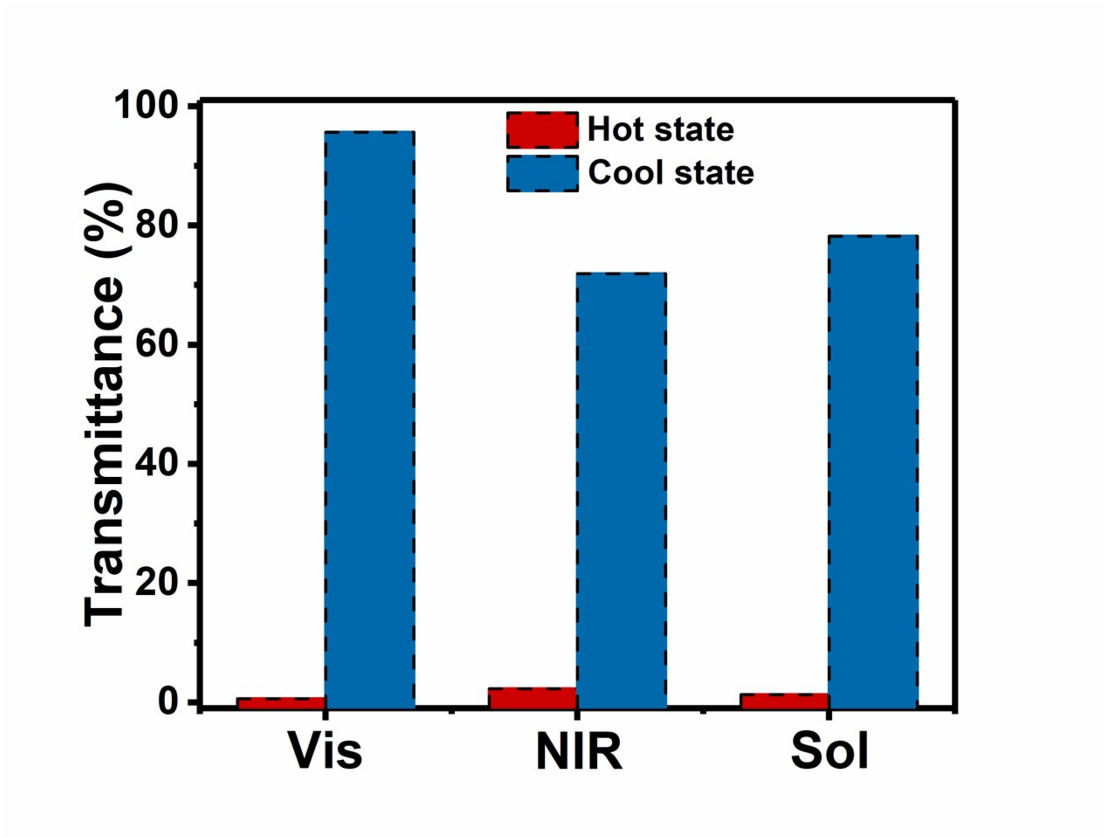

Figure S18. Transmittance to visible, near-infrared, and solar of the PNASW at cool and hot states.

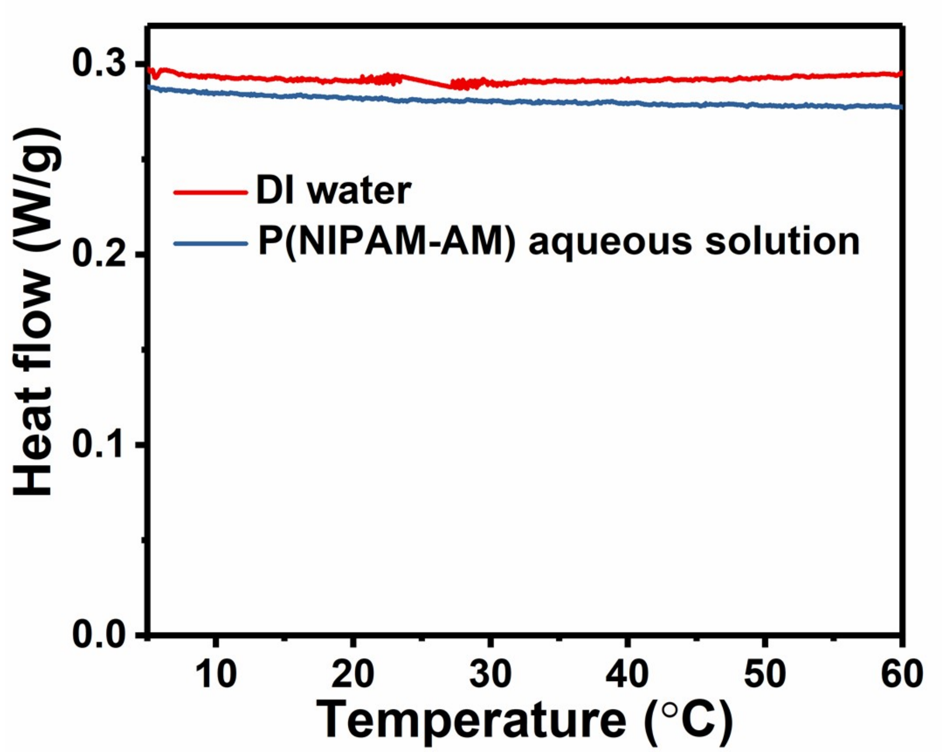

Figure S19. DSC curves for P(NIPAM-AM) aqueous solution and DI water for the temperature range of 5~60°C.

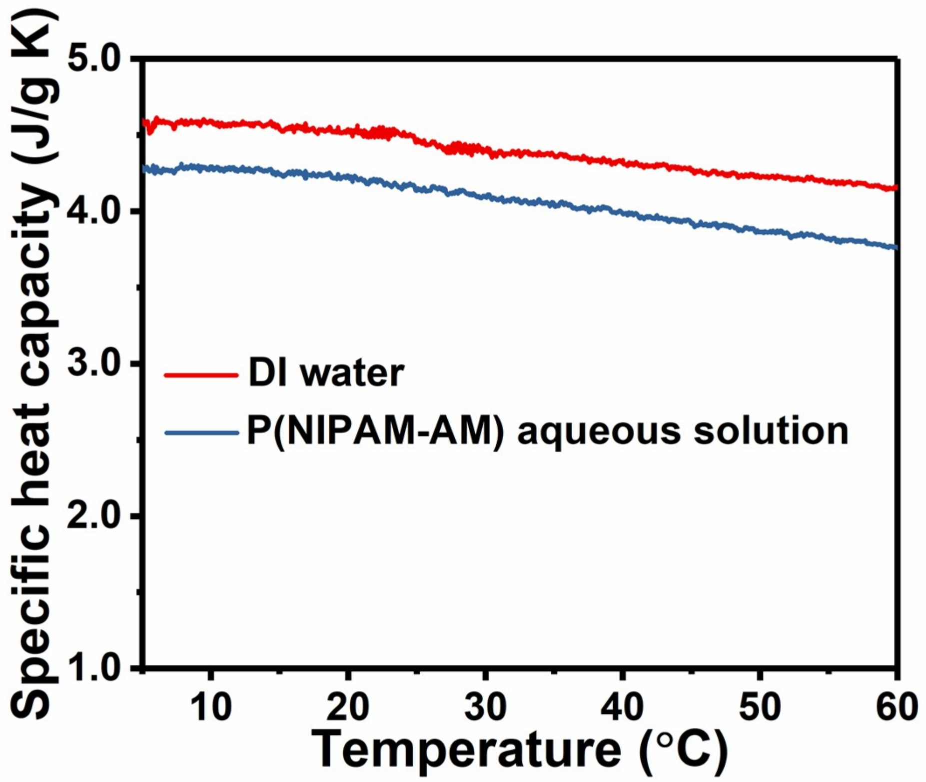

Figure S20. Specific heat capacity curves for P(NIPAM-AM) aqueous solution and DI water for the temperature range of 5~60°C.

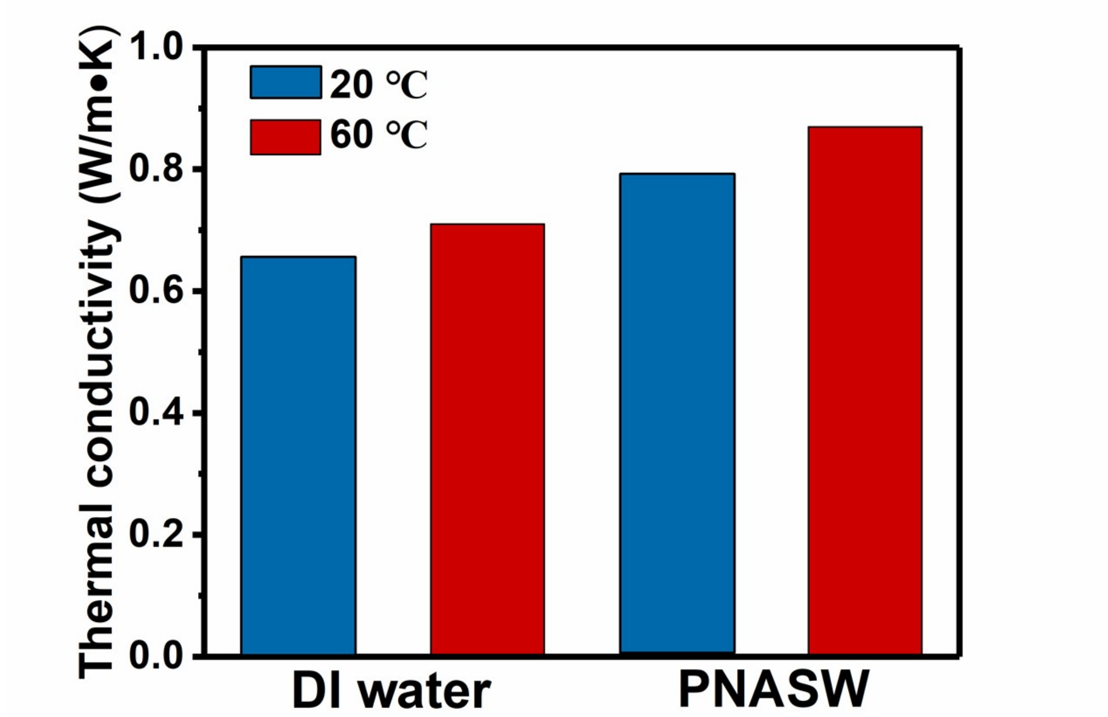

Figure S21. Thermal conductivity of P(NIPAM-AM) aqueous solution and DI water at RT and HT.

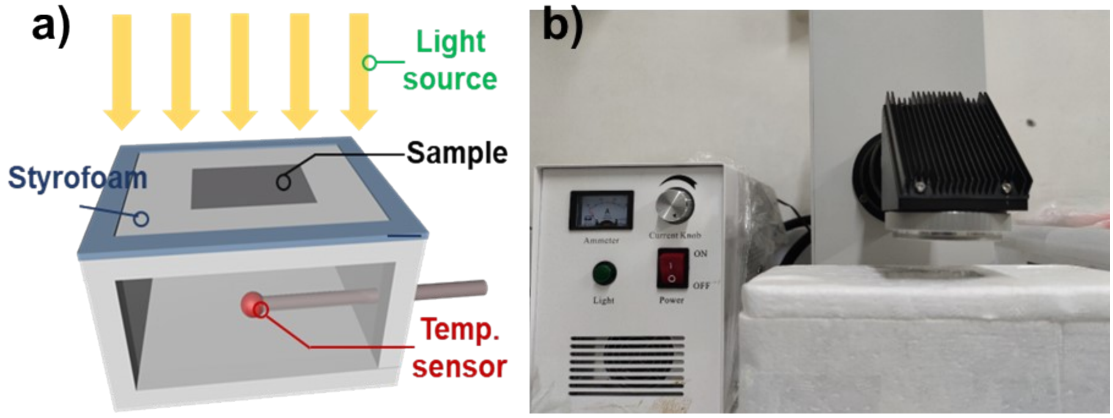

Figure S22. a) Building-model for temperature insulation tests; b) Digital image of the xenon lamp with a power of 30 W.

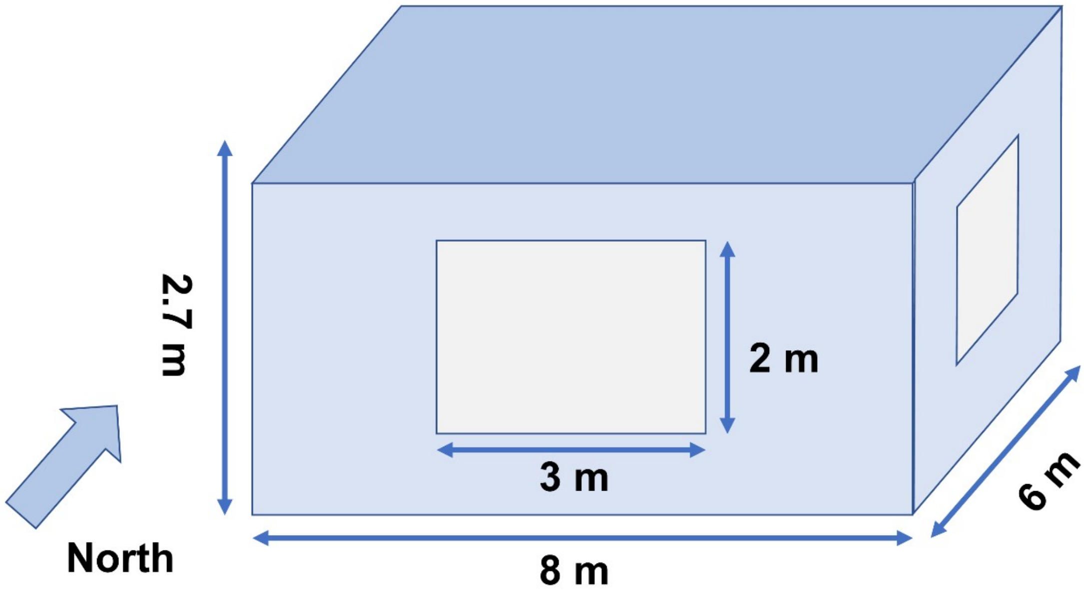

Figure S23. Building model constructed for energy-saving simulation.

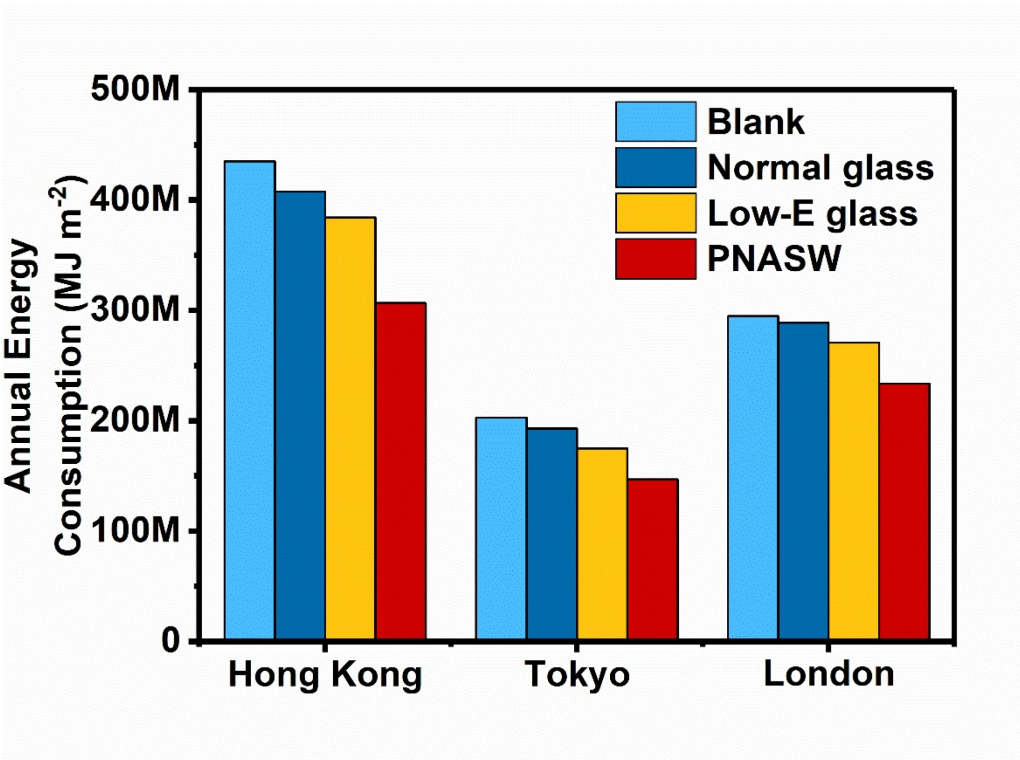

Figure S24. Annual energy consumption of the building model with four samples at Hong Kong, Tokyo, and London.

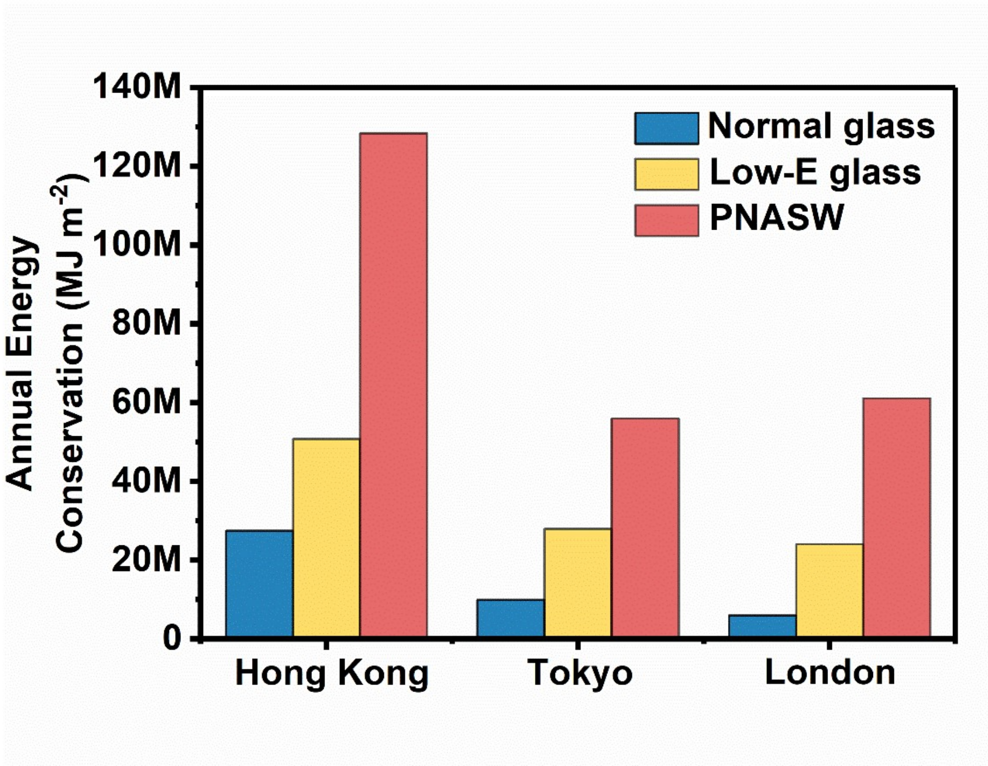

Figure S25. Annual energy conservation of the building installed with normal glass, low-E glass, and the PNASW compared to the direct solar radiation.

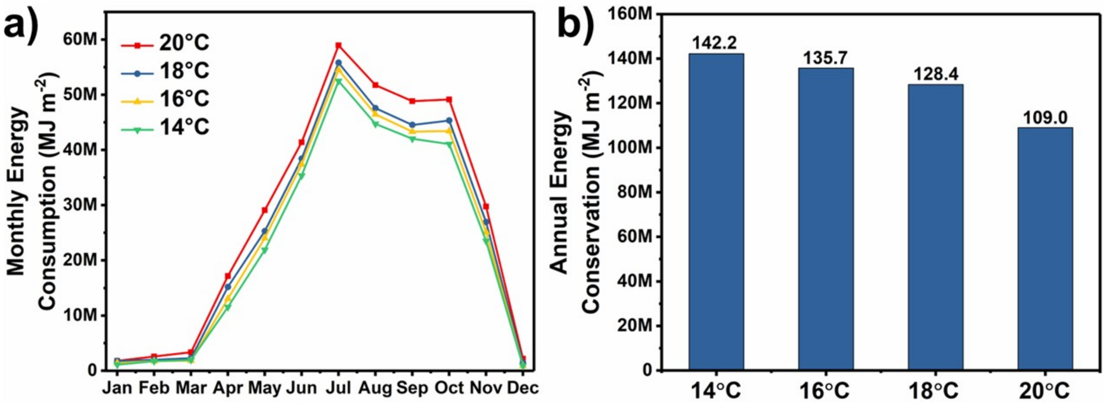

Figure S26. a) Monthly HVAC energy consumption and b) annual energy conservation of PNASW with different responsive temperatures in Hong Kong.

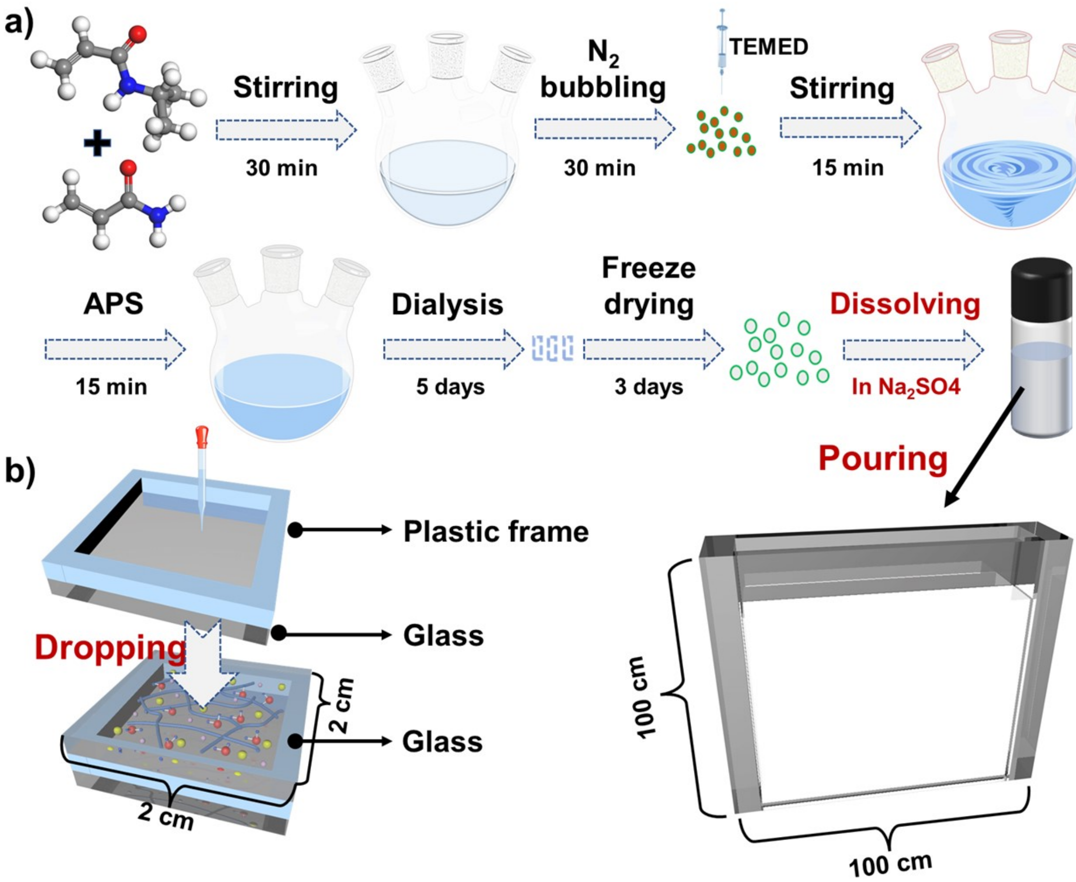

Figure S27. The schematic fabrication process of a) P(NIPAM-AM) and b) the PNASW.

Table S1. The length and total energy of H-bonds obtained by DFT calculation.

<table>
<tr><td>Monomer</td><td>H-bond length (Å)</td><td>Average length (Å)</td><td>Binding energy (kcal mol^{-1})</td><td>Total energy (kcal mol^{-1})</td></tr>
<tr><td rowspan="3">NIPAM</td><td>1.920</td><td rowspan="3">2.002</td><td>-5.759</td><td rowspan="3">-17.338</td></tr>
<tr><td>1.979</td><td>-6.661</td></tr>
<tr><td>2.106</td><td>-4.918</td></tr>
<tr><td rowspan="4">AM</td><td>1.442</td><td rowspan="4">1.439</td><td>-4.452</td><td rowspan="4">-22.874</td></tr>
<tr><td>1.587</td><td>-5.257</td></tr>
<tr><td>1.505</td><td>-6.205</td></tr>
<tr><td>1.221</td><td>-6.960</td></tr>
<tr><td>Dimer</td><td>H-Bond length (Å)</td><td>Average length (Å)</td><td>Binding energy (kcal mol^{-1})</td><td>Total energy (kcal mol^{-1})</td></tr>
<tr><td rowspan="6">$PNIPAM_2$</td><td>1.951</td><td rowspan="6">1.863</td><td>-5.746</td><td rowspan="6">-42.181</td></tr>
<tr><td>1.891</td><td>-4.909</td></tr>
<tr><td>1.910</td><td>-7.955</td></tr>
<tr><td>1.825</td><td>-5.846</td></tr>
<tr><td>1.909</td><td>-7.878</td></tr>
<tr><td>1.694</td><td>-9.847</td></tr>
<tr><td rowspan="7">$P(NIPAM\text{-}AM)_2$</td><td>1.775</td><td rowspan="7">1.854</td><td>-6.954</td><td rowspan="7">-49.610</td></tr>
<tr><td>2.010</td><td>-5.329</td></tr>
<tr><td>1.809</td><td>-9.066</td></tr>
<tr><td>1.721</td><td>-7.923</td></tr>
<tr><td>1.856</td><td>-6.687</td></tr>
<tr><td>1.922</td><td>-6.003</td></tr>
<tr><td>1.883</td><td>-7.648</td></tr>
</table>

Table S2. LCST of P(NIPAM-AM) in different salts and their corresponding fitting formulas (y is the LCST and x is the concentration of salt).

Salt (0~0.5 M)	Adjustable range	Salting in/out	Fitting formula (x = concentration, y = LCST)	R^2	HEI (k)
Na_2SO_4	-45.0℃	Out	$y = -89.14x+53.62$	0.999	-89.14
Na_2CO_3	-41.2℃	Out	$y = -81.71x+53.43$	0.998	-81.71
NaCl	-7.1℃	Out	$y = -14.43x+53.85$	0.985	-14.43
NaBr	-2.4℃	Out	$y = -5.11x+54.10$	0.981	-5.11
$NaNO_3$	-1.9℃	Out	$y = -4.03x+54.09$	0.979	-4.03
E325	-9.5℃	Out	$y = -19.29x+53.90$	0.998	-19.29
NaAc	-12.3℃	Out	$y = -23.71x+54.09$	0.995	-23.71
$ZnSO_4$	-19.4℃	Out	$y = -38.89x+53.84$	0.999	-38.89
$MgSO_4$	-36.5℃	Out	$y = -72.31x+54.59$	0.999	-72.31
$(NH_4)_2SO_4$	-31.2℃	Out	$y = -62.60x+53.93$	0.999	-62.60
$CuSO_4$	-29.5℃	Out	$y = -61.57x+54.48$	0.997	-61.57
$KHSO_4$	-18.5℃	Out	$y = -36.86x+54.64$	0.994	-36.86
$FeSO_4$	-32.3℃	Out	$y = -64.49x+53.70$	0.999	-64.49
NaI	+3.8℃	In	$y = 7.11x+54.30$	0.968	+7.11
$CaCl_2$	-6.3℃	Out	$y = -11.77x+54.28$	0.981	-11.77
$Ca(NO_3)_2$	From +2.1 to -1.2℃	In/out	$y = -32.14x^2+13.50x+54.07$	0.911	\
$MgCl_2$	-5.2℃	Out	$y = -10.29x+54.04$	0.999	-10.29
$Mg(NO_3)_2$	From +3.3 to +1.8℃	In/out	$y = -26.07x^2+16.24x+54.06$	0.907	\
NaSCN	+6.2℃	In	$y = 13.02x+54.03$	0.997	+13.02

Table S3. Parameters of the window samples used for the energy consumption simulation

Name	Normal glass	Low-E glass	PNASW	
			Cool state	Hot state
Solar transmittance	95.1%	71.4%	78.2%	1.3%
Solar reflectance	3.5%	5.8%	5.5%	20.4%
Visible transmittance	98.7%	69.8%	95.6%	0.6%
Visible reflectance	2.1%	6.7%	4.4%	18.6%
Front Side Infrared Hemispherical Emissivity	87.6%	94.8%	87.6%	87.6%
Back Side Infrared Hemispherical Emissivity	87.6%	39.7%	51.4%	32.3%
Conductivity (W/m·K)	0.92	0.92	0.79	0.87